ESTIMATING THE EFFECT OF GREEN ROOFS ON A CITY'S ENERGY FOOTPRINT

TG Myers*, ND Fowkes†, AG Fareo‡ and S Goqo⋆

Industry Representatives

A Fitchett[1] and A G Fareo

Study Group participants

T Holtzhausen, HM Mamboundou and N Mewalal

Abstract

The temperature generated (and hence energy stored) in a solid layer subjected to sunshine is examined. Two models are developed which permit the calculation of the temperature from the surface to far into the ground. By varying parameters we can replicate heat flow in soil or concrete, there is also the option to include evaporation and evapotranspiration. The results obtained indicate that significant temperature reductions and energy storage in the solid layer can be achieved by a sensible choice of roof covering and composition. The models are one-dimensional but it is a simple matter to extend the calculations to deal with a patchwork quilt of surfaces as would be present in a city. Recommendations are given to reduce heat storage in a city and also on future model improvements.

1 Introduction

Close to 55% of the world's population is living in urban areas or cities. According to a United Nations report [1], it is predicted that by the year 2050, two-thirds of the global

*Centre de Recerca Matematica, Barcelona, Spain. *email: myerscrm@gmail.com*

†Mathematics Department, University of Western Australia, Crawley, WA 6009, Australia *email: neville.fowkes@uwa.edu.au*

‡School of Computer Science and Applied Mathematics, University of the Witwatersrand. *email: adewunmi.fareo @ wits.ac.za*

⋆School of Mathematics, Statistics and Computer Sciences, University of KwaZulu-Natal. *email: goqos@ukzn.ac.za*

[1]Assistant Dean, Faculty of Engineering and the Built Environment, University of the Witwatersrand. *email: anne.fitchett@wits.ac.za*

population will live in urban areas, resulting in higher levels of densification. The increase in inhabitants has led to urban sprawl, mostly in developing countries [2]. This has led to the spread of urban areas into farmlands, causing farm reclamation and deforestation activities. When the vegetative spaces, like farmlands are turned into urban structures, there is often an associated rise in temperature, a phenomenon first noticed in London in the 19th century [3] and referred to as the urban heat island effect. It has been recognised that the temperature difference is primarily due to the absorption of radiation by concrete, bitumen, and the roofs that make up the city compared with vegetation in the nearby countryside. Human activities in the city also affect urban temperatures, contributing to the heat island effect. Factories normally produce heat and carbon dioxide and other emissions which affect the heat balance. Buildings in cities block winds, thus reducing the heat transport rate. Human beings themselves also produce heat. Clearly there are many factors that contribute to the greater retention of heat in cities; for more details see Nuruzzaman [28].

Since its detection, there has been numerous observations of heat islands in urban areas and cities around the world. Urban heat islands are most noticeable at night during clear weather and with low winds and while they are most problematic for human beings during summer periods, their effect is most pronounced during winter [4]. These studies have established that a correlation exists between an increase in green areas and a decrease in local ambient air temperatures [4, 5, 6, 7, 8, 9, 10, 11]. By monitoring the urban heat island in four areas of New York City, Susca et.al. [10] found an average of 2°C difference between the most and the least vegetated areas.

Various forms of greenery can exist in urban areas, including parklands, gardens, greenroofs, planting of extensive vegetation, nature reserves etc, all acting as sources of moisture for evapotranspiration, a process whereby solar radiation is converted to latent heat. However, since in densely populated urban areas there are few unused spaces that can be transformed into green areas, a viable solution to mitigate the urban heat island effect is to convert traditional roofs into green/vegetative roofs. Roofs make up about 20-25% of the urban surface area [12] and their conversion to green roofs is relatively inexpensive, so that such conversion may be the most cost effective way of controlling climate change in urban areas. Coakley [14] presented different albedos for different surfaces such as oceans, lakes, concrete, asphalt and forests which have low albedos and snow, sea ice and deserts which have large albedos. Low albedo materials contributes to worsening of the urban heat island formation [15]. Sodoudi et al. [16] studied the effects of greenery in connection with the high albedo materials in reducing the urban heat island effect in the metropolitan area of Tehran. In this study, a higher cooling effect in the daytime was observed.

Different studies and models in the past have focused on understanding the factors that affect the temperature in urban heat-islands [15, 17, 18, 19, 20, 21]. Bennett and Saab [22] made a review of the physical processes of urban atmospheres using the advection-diffusion equation and physical modelling in wind tunnels. Atkinson [23] used a three-dimensional, non-hydrostatic numerical model to analyse urban heat-island intensity. The model for an urban area of 20 km^2 included albedo, heat flux, emissivity, roughness length, sky–

view factor,surface resistance to evaporation and thermal inertia. It was discovered that these properties made varying contributions to the causes of daytime and night time urban heat-islands. In daytime the roughness length and surface resistance to evaporation were the most important factors affecting urban heat–island intensity, at night the heat was the most important. The Weather Research and Forecasting model was tested in Greece by Giannaros [24] et al. The main findings from this study revealed that the city's surface temperature was higher than its surroundings in the nighttime. Nazarian et al. [25] conducted numerical modeling of outdoor thermal comfort and concluded that approximations of surface temperature found in existing thermal models are not suited for high–density urban areas. A recent study by Meili et. al. [26] focused on an urban ecohydrological model which looked at the effect of vegetation on urban climate and hydrology. The model was able to account for the effects of different plant types and urban–green typologies. It also provided information on how the urban environment affects plant well–being and performance.

The aim of this project is to determine if the greening of roofs in the cities could make a significant difference to urban heating, and if this difference would be such that cities should consider introducing regulations or incentives that would encourage owners to 'green their roofs'. Of course there are major engineering, economic and social issues that would need to be taken into account when considering introducing regulations or incentives. Here we will focus on the physics and leave the more complex social questions to our economics colleagues and political masters.

It is recognised that the increased temperature levels seen in cities are very dependent on its location, climate and geography and of course the time of day, so that any 'generic evaluation' of the effect of greening roofs needs to filter out such issues; such issues would certainly need to be examined for specific circumstances. For this reason we consider the simple situation in which solar radiation falls on a horizontal surface. The effect of colour and composition on the surface temperature and net heat absorption over a typical day is of interest here. The effect of using plants/groundcover is of course of special interest to us. The model could be extended to deal with a patchwork of surfaces, as is the case in the city.

There has been a vast amount of work done on this problem (social, political..) but little of it is 'technical'; we will not attempt to detail the social and political work. Rather our concern will be with the physics. Some computational results have been obtained in a particular case, see Myrup [30], but such investigations are of limited applicability and shed little light on the general question of interest here.

In Section 3 we will set up a simple 1D model corresponding to the radiative heating of a horizontal surface (the Earth). Linear approximations are introduced and exact solutions are obtained using a Laplace transform technique. An alternative Green's function/boundary integral approach for proceeding to solution is developed in Section 4.3. This formulation is likely to be useful for non-linear and time varying heat transfer situations. Results are presented in Section 4 and conclusions are drawn in Section 5. First, however, in Section 2 we will present background work on transpiration.

2 Absorption and transpiration: the Penman-Monteith equation

The effect of vegetation on heat transport is twofold:

- Firstly the albedo is greatly reduced because much of the incoming radiation is multiply reflected and absorbed between the leaves of the plants, leading to a much increased heat absorption within the foliage. Rosseland [32], [33] approximations may be used to determine the effective (temperature dependent) 'conductivity' of a plant layer but for our purposes we simply use experimentally determined values for the albedo. Typical values are 0.2 for vegetative surfaces compared with 0.35 for normal soil, see Table 3

- Secondly there is the effect of transpiration. Much of the radiation absorbed within the vegetation causes evaporation from the large surface area of leaves, and it is the associated latent heat absorption that underlies the effectiveness of plant cover. This evaporation rate is measured in terms of an equivalent depth change of a free water surface, and typical values for a crop of barley weed are $\dot{d} = 1 - 3$ mm per day, and 7.2 mm/day for rice in a paddy [34]. The associated heat absorption rate is of interest here and is given by $L_f \dot{d} \rho_w$ per unit surface area, where L_f is the (water/steam) latent heat (J/m^3) and ρ_w the density of water. Typically the associated 'surface temperature' reduction is about 2.5 C°. Agriculturists have long been interested in such issues and models have been developed to determine the effect of climate on evaporation rate in the short and long term. We briefly describe the botany and the models.

Plants act as a conduit for the transport of water from the soil to the atmosphere. In the absence of sunlight guard cells close the stomatal cavities in the leaves so that moisture is not lost. The evaporation rate is thus (almost) zero when the sun goes down. (These guard cells also close the cavity under extreme heat stress to prevent moisture loss.) During daylight the guard cells 'relax' so that stomata open, and the resultant (diffusive) moisture transport rate is proportional to the difference in moisture potential between the stomatal cavities (the air filling the cavity is essentially at the saturation moisture level at the leaf temperature) and that of the immediate environment of the plant leaves, which in turn is determined by the temperature and humidity of the external environment. Since air currents transport moisture away from the leaves the wind speed affects moisture transport. Soil moisture levels also affect transpiration rates. The system is thus coupled and complex. It should be noted that photosynthesis (carbon dioxide absorption) can only occur if the stomata are open, so plant growth requires transpiration.

The Penman-Monteith equation approximates the evapotranspiration as a function of the climatic conditions (solar radiation, air temperature, relative humidity and wind speed) and the leaf and canopy characteristics (stomatal conductance, boundary layer and aerodynamic conductance). This theory was initially developed to determine average

evapotranspiration over a day or longer but has been adapted to describe hourly averages. The theory is based on the observations described above with resistances introduced to describe the heat and water vapour flux from the stoma through the aerodynamic boundary layer and then into the external environment. The model assumes that the crop is well watered so that soil flow resistance is not an issue. The theory determines the volume flux of water per unit surface area due to evapotranspiration, (E/ρ_w), or simply 'the evaporation rate' $\dot{d}$, as

$$\dot{d} = \frac{\Delta(Q_n - G) + \rho_a c_p(\delta e) g_a}{(\Delta + \gamma(1 + g_a/g_s))L_v} \equiv \left[\frac{(Q_n - G)}{L_c}\right]\left[\frac{1 + \frac{\rho_a c_p}{(Q_n - G)} g_a \delta e_s}{1 + \frac{\gamma}{\Delta}(1 + \frac{g_a}{g_s})}\right], \tag{1}$$

with the associated latent heat flux density given by $L_v\dot{d} \equiv L_f \rho_m \dot{d}$, where L_f (J/kg) is the latent heat of vaporisation, and $L_v = L_f\rho_m$ is referred to as the volumetric latent heat of vaporization of water ($L_v = (2453 \times 10^6 \mathrm{Jm}^{-3})$, see [35, 37]. Here:

$\dot{d}$	=	Water volume transpired (per unit surface area) per sec. (m s^{-1})
Q_n	=	Net irradiance of the external source of energy flux (W m^{-2})
G	=	Net ground heat flux per unit surface area (W m^{-2})
Δ	=	Rate of change of saturation specific humidity with air temperature (Pa K^{-1})
c_p	=	Specific heat capacity of air (J kg^{-1} K^{-1})
ρ_a	=	Dry air density (kg m^{-3})
δe	=	Vapour pressure deficit or specific humidity of air (Pa)
g_a	=	Conductivity of air (m s^{-1})
g_s	=	Conductivity of stoma (m s^{-1}).
γ	=	Psychrometric constant ($\gamma =$ 66 Pa K^{-1})

Note that the net irradiance Q_n as used above is defined by

$$Q_n = Q_s(1 - \mathcal{A}) \,, \tag{2}$$

where Q_s is the total radiative power per unit area arriving on the surface in the absence of reflection, and $\mathcal{A}$ is the albedo, determined by the colour and nature of the surface. This net power input drives evapotranspiration and heat transfer into the atmosphere and heat flow into the Earth. The vapour pressure deficit is defined by

$$\delta e = e_s(T_a) - e_a \equiv e_s(T_a)RH, \tag{3}$$

where e_a is the actual (environmental) vapour pressure above the canopy and $e_s(T_a)$ is the saturated vapour pressure at the environmental temperature T_a; RH is the relative humidity. Any deficit will result in moisture transport. Note that the total transpiration of a leaf/canopy is modelled as the sum of two terms; a net radiative input term, and a 'local' (diffusive, convective) vapour transport term, see Equation 1. The second expression in (1) more clearly displays the significant groups effecting the evaporation rate. Evidently the evaporation rate increases (almost) in proportion to the net radiative input $(Q_n - G)$

with higher evaporation levels at higher environmental temperatures and humidities. It should be noted the aerodynamic conductivity g_a is strongly dependent on wind speed, as described by additional turbulent flow models, see later .

The saturated vapour pressure $e_s(T_a)$ is an exponential function of temperature determined using the Clausius-Clapeyron relation, which is well approximated by the August-Roche-Magnus equation

$$e_s(T) = 0.61 \ \exp^{\frac{17.625 \ T}{T+243}}, \tag{4}$$

see [39, 40], where T is in C°, and e_s is in k Pa. Figure 1 Left displays the (surface) temperature dependence of the saturated vapour pressure over the temperature range of interest; it changes from 2.3 kPa at 20 C°, to 7.38 kPa at 40 C° which strongly effects evaporation rates. Note however that this relationship is almost linear in temperature, an approximation used in deriving the Penman-Monteith equation and also used in Section 3.

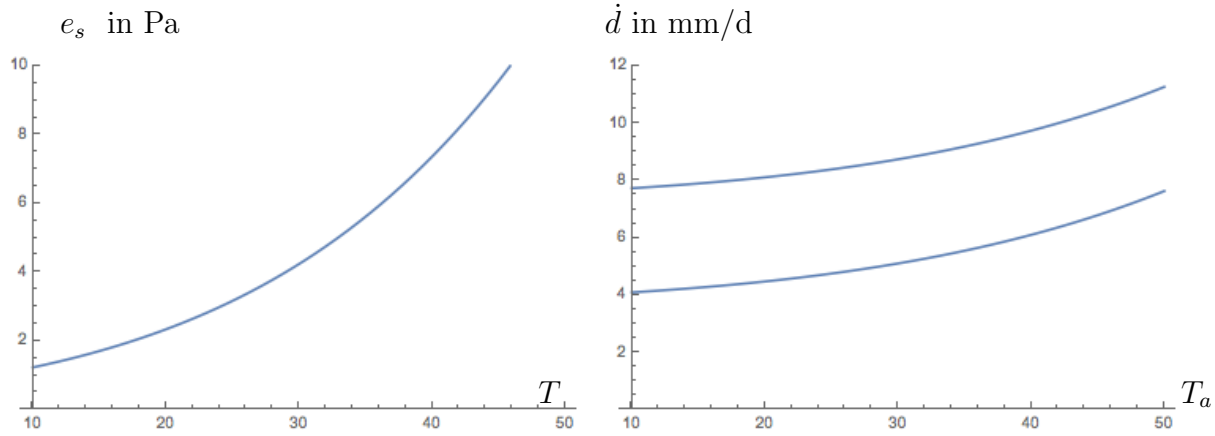

Figure 1: Left: Clausius-Clapeyron equation: saturated vapour pressure $e_s(T)$ (Pa) changes with temperature $T(°\text{C})$. Right: Evapotranspiration rate $\dot{d}_0$ (mm/day) for the reference crop as a function of the air temperature $T_a(°\text{C})$ above the crop. The net radiative heating $(Q_s - G)$ is 1000 W/m^2 (upper curve) and 500 W/m^2 (lower curve). The wind speed is 1 m/s and the humidity is at 50%.

The Penman-Monteith equation has evolved over the past 50 years, and other simpler/more easily used models have been suggested. For example the Priestly-Taylor model uses empirically determined constant factors to avoid the measurement of aerodynamic terms, but such approximations are of limited use. We will stick with the Penman-Monteith equation. It has been found that there are large local variations (in conductance parameters mainly) and so agreed guidelines have been set up to produce a reference crop evapotranspiration model based on an excellently managed, uniform height, well watered field of grass, see [38]. This hypothetical reference crop, referred to as the *the reference crop*, is grass of uniform height 0.12 m, having a surface conductance of 70 sec m^{-1} and an albedo $\mathcal{A} = 0.23$, see [38] for details. The environmental parameters for this crop are measured at a height 2 m above the ground. The approximated parameter values

for this reference crop are displayed in Table 1. Note that stress coefficients are used to account for reductions in evapotranspiration due to environmental stress (unsaturated soil, pollution effects etc).

Aside: The aerodynamic resistance model used is the von Karman turbulence model. Explicitly the aerodynamic resistance $r_a = 1/g_a$ is given by

$$r_a = \frac{\ln\left[(z_m - d)/z_{0m}\right] \ln\left[(z_h - d)/z_h\right])}{\mathcal{K}^2 u_2},$$

where z_m (2 m) is the height of the wind measurements, $z_h = 2$ m is the height of the humidity measurements, z_{0m} (m) is the roughness length taken as $z_{0m} = 0.123 z_h$, d is the zero plane displacement height taken as $(2/3\ z_h)$ m, and $\mathcal{K}$ is von Karman's constant (0.41). This model can be used to describe the vapour transport under windy conditions, but cannot be used to describe the transport under no wind conditions; an additional vapour transport term needs to be added in. The bulk surface resistance ($r_s = 1/g_s$) used is

$$r_s = r_l / LAI,$$

where r_l is the stomatal resistance of a well illuminated leaf (s m^{-1}) and LAI is the active leaf area index given by the ratio of the leaf area (upper surface only) over the underneath soil surface area; Typical values are 3 to 5. For more details concerning the reference crop see [38].

Since our aim is to evaluate the effect of greening on temperature under 'general conditions' it makes sense to work with this reference crop, especially since roofs are likely to be cropped with grasses or dense vegetation. (Modifications may be added in as needed for 'non-ideal' situations but will not effect the qualitative results we obtain.)

Results for the evaporation rate in mm/day for the standard crop as a function of 'net' surface heating $(Q_n - G)$, and the environmental temperature T_a are presented in Figure 1 Right. Here we have assumed that: the net surface heating is at 1000 W/m^2 and 500 W/m^2, that the air above the crop is at 50% humidity, and that there is a wind speed of 1 m/sec. Note that the 'net' surface heating subtracts out the ground flux G from the radiative heating rate Q_s. This ground heat flux will be determined in the next section. The results shown in the figure indicate a evapotranspiration rate of about 4-10 mm/day, which matches observations. Note that the evaporation rate increases (almost) in proportion to the radiative input, and increases rapidly with wind speed and environmental temperature. It is worth noting that the evaporation rate increases almost linearly with temperature (with an offset), which justifies the approximate work of Section 3.

3 Heat flow into the Earth: the governing equations

The radiative energy from the sun acts to heat up the ground. Obviously the effect is greatest near the surface. During the day this heat will be conducted downwards, away

$r_a = 1/g_a$	$208/u_2$ s m^{-1}
$r_s = 1/g_s$	r_l/LAI s m^{-1}
$r_l = 1/g_l$	100 s m^{-1}
$r_s = 1/g_s$	70 s m^{-1}

Table 1: Parameter values used for the *reference crop*: r_l is the leaf resistance, LAI is the leaf area index, u_2 is the wind speed.

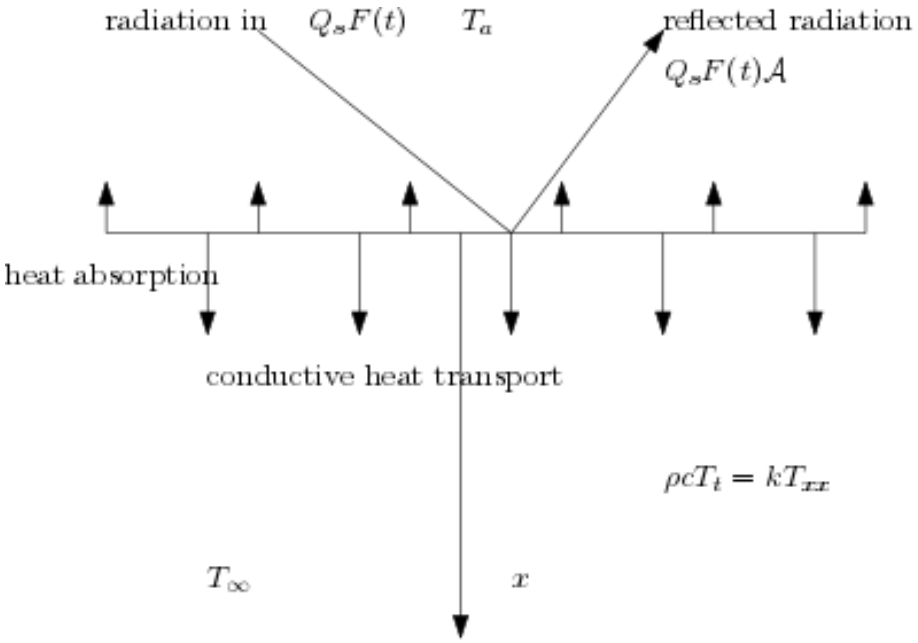

Figure 2: Radiation into a conducting half space: Part of the incoming radiation is reflected ($\mathcal{A}Q_sF(t)$) and the remainder is either lost through evaporation or conducted into the lower half-space.

from the surface, typically penetrating to around 50 cm (see the scaling discussion in §3.2). The thermal energy captured by the ground during the day will be stored and released at night when the air temperature is lower than that of the surface, and there is no net radiative input. Note, approximately 10 m below the surface the average temperature is constant throughout the year and dependent upon the latitude and soil type. Closer to the surface the average temperature varies slowly with the daily average.

In this section we will write down a one-dimensional mathematical model to describe the variation of the ground temperature during daylight hours. The analysis can then indicate the effect of parameter values on the temperature and energy storage. If we wish to use it to calculate the energy over a given area of land (subject to the same heating conditions) then we can simply multiply by the surface area.

The temperature in a one-dimensional solid layer is governed by the heat equation

$$\rho c \frac{\partial T}{\partial t} = k \frac{\partial^2 T}{\partial x^2} \ .$$

For the present situation we assume that the upper surface is exposed to the sun which acts to heat up the ground. Thermal energy may be returned to the air through radiation and convective heat transfer. In the case of a green roof energy is also lost due to evaporation or transpiration, as discussed in the previous section. During daylight hours the energy flux into the surface $x = 0$ is then comprised of the heat gain via the sun and the three heat loss terms

$$-k\frac{\partial T}{\partial x} = (1-\mathcal{A})Q_s - \epsilon\sigma(T^4 - T_a^4) - H(T - T_a) - \rho_w L_f \dot{d} = Q_{in}, \tag{5}$$

where L_f is the latent heat of water, $\dot{d}$ is the volumetric evaporation rate per unit area. Note for later purposes that Q_{in} defines the net 'external power input' into the surface. Typical parameter values are given in Table 2.

It is standard to simplify the radiation term by assuming the surface temperature is close to the air temperature (in Kelvin we expect changes of the order 10-20%).

Linearizing the radiation term gives

$$-k\frac{\partial T}{\partial x} = (1-\mathcal{A})Q_s - (H + 4\epsilon\sigma T_a^3)(T - T_a) - \rho L_f \dot{d}\ .$$

The initial and far-field temperatures are set to the average temperature over a 24 hour period,

$$T(x,t)\Big|_{x\to\infty} \to T_{av}\ , \qquad T(x,0) = T_{av}\ .$$

3.1 Relation to Penman-Monteith equation

Noting that $G = -kT_x$ is the heat flux from the soil we may write the Penman-Monteith equation (1) in the form

$$-k\frac{\partial T}{\partial x} = Q_n + \frac{\rho_a c_p g_a \delta e}{\Delta} - \rho_w L_f \dot{d}\left[1 + \frac{\gamma(1 + g_a/g_s)}{\Delta}\right]\ .$$

Teten's approximation for the saturated vapour pressure gives

$$e_s = 610 e^{17.27(T-273.15)/(T-35.85)}\ .$$

This is identical to the form provided in the previous section, except the temperature is now expressed in Kelvin and e_s is in Pa. Then $\delta e \approx e_s(1 - RH/100)$ where the relative humidity RH is a percentage. Other terms may be replaced by the relations

$$1 + \frac{g_a}{g_s} = 1 + 0.34u_2\ , \qquad c_a\rho_a g_a = \frac{900\gamma u_2}{T}\ , \tag{6}$$

$$\Delta = \frac{4098 e_s}{(T - 35.85)^2}\ , \qquad Q_n = (1-\mathcal{A})Q_s\ , \tag{7}$$

where u_2 is the wind speed 2m above the soil. Hence

$$-k\frac{\partial T}{\partial x} = (1-\mathcal{A})Q_s + \frac{900\gamma u_2}{T}\left(1-\frac{RH}{100}\right)\frac{(T-35.85)^2}{4098} - \rho_w L_f \dot{d}\left[1+\frac{\gamma(1+0.34u_2)}{\Delta}\right] .$$

All of these definitions are discussed in more detail in [27]. The Penman-Monteith equation may thus be seen as a correction to the standard heat flux model, accounting for the more complex behaviour of plants in a warm environment (as compared to a solid surface). The final term on the right hand side coincides with the heat loss due to evaporation in (6) but with a correction to account for the mass loss from the stomata to the air. The second term, proportional to the temperature replaces the heat loss due to radiation from the surface and convective heat transfer.

In the limit $u_2 = 0$

$$-k\frac{\partial T}{\partial x} = (1-\mathcal{A})Q_s - \rho_w L_f \dot{d}\left[1+\frac{\gamma}{\Delta}\right] .$$

In the absence of wind both convective heat transfer and radiation back to the atmosphere still occur, but they are not accounted for in the above equation. This demonstrates an incompatibility between the forms. Equation (6) is a standard form for a solid surface, while equation (8) is standard for evapotranspiration. The two models do not coincide as the amount of vegetation or wind speed decrease. A more complete study we will require both types of condition when comparing vegetated and non-vegetated roofs (or some corrections terms added to both equations).

Finally, we may estimate the evaporation rate by noting that the heat flux from the soil is significantly less than the incoming radiation $G \ll Q_s$ and so

$$\dot{d} \approx \frac{(1-\mathcal{A})Q_s}{\rho_w L_f\left(1+\frac{\gamma}{\Delta}\right)} .$$

With $Q_s = 800$ W/m^2, $\mathcal{A} = 0.4$, $\gamma = 66$ Pa/$^\circ C$, $\Delta = 240$ Pa/$^\circ C$ we find

$$\dot{d} = 1.7\times 10^{-7} \text{ m/s} \approx 6 \text{ mm/day}$$

assuming a day involves eight hours of (strong) sunlight. This is the water loss rate that would occur with a well watered field containing the reference crop (sward grass of height 0.12 m). For arid or semi-arid conditions predictions are much lower. In [27] values ranging between 1 and 2 mm/day are quoted for the four models investigated (including Penman-Monteith), and this is consistent with the results of Section 2. Assuming green roofs in Johannesburg are not composed of well watered long grass we will take an intermediate value of 4 mm/day in the following calculations.

3.2 Non-dimensional system

We define non-dimensional variables such that

$$\hat{T} = \frac{T-T_{av}}{\Delta T} , \qquad \hat{x} = \frac{x}{L} , \qquad \hat{t} = \frac{t}{\tau}$$

and immediately drop the hats.

The heat equation and boundary conditions may now be written

$$\begin{aligned} & \frac{\partial T}{\partial t} &=& \frac{\partial^2 T}{\partial x^2} \,, \\ x = 0: \qquad & -\frac{\partial T}{\partial x} &=& 1 - T \,, \\ x \to \infty: \qquad & T &\to& 0 \,. \end{aligned}$$

These require choosing

$$\begin{aligned} \tau &= \frac{\rho c L^2}{k} \,, \qquad L = \frac{k}{H + 4\epsilon\sigma T_a^3} \,, \\ \Delta T &= \left[(1-\mathcal{A})Q_s - (H + 4\epsilon\sigma T_a^3)(T_{av} - T_a) - \rho_w L_f \dot{d}\right] \frac{L}{k}. \end{aligned}$$

The choice here is made with the assumption that T_a, $\dot{d}$ are constant. Strictly speaking we are now working with an approximation valid for relatively short time-scales where the ambient temperature and evaporation rate are approximately constant. A model valid for longer times may be easily written down, using the above scales, but with T_a, $\dot{d}$ taken as some typical daily value and then small terms representing the variation from these values will enter the boundary condition at $x = 0$. For the present we will stick with the simple, constant model (adding the variation is an obvious extension to future work). Using the parameter values of Table 2 indicates that for concrete the temperature scale $\Delta T \approx 11°$C, length-scale $L \approx 5$ cm and time-scale $\tau \approx 2$ hours. That is, if the sun shone constantly onto a concrete surface for 2 hours we could expect temperature rises of the order 11°C and the heat will penetrate to the order 5 cm. (These are consistent with the numerical results presented later, which show a maximum temperature rise of around 6°C and a penetration of 20 cm after 2 hours). Similar values are obtained for soil.

Q_s	800	W/m^2	T_{av}	293	K
$\mathcal{A}_c$	0.4		$\mathcal{A}_s$	0.2	
T_a	298	K			
ϵ	0.9		σ	5.7×10^{-8}	W/m^2 K^4
ρ_w	1000	kg/m^3	ρ_c	2400	kg/m^3
k_c	0.8	W/(mK)	c_c	880	J/kg/K
ρ_s	1510	kg/m^3			
k_s	0.864	W/(mK)	c_s	1000	J/kg/K
H	10	W/m^2/K	$\dot{d}$	1.11×10^{-7}	m/s
L_f	2.26×10^6	J/kg			

Table 2: Typical parameter values [31, 36, 41],

asphalt	0.05-0.15	agricultural crops	0.18-0.25
concrete	0.25-0.7	grass	0.16-0.25
soil (sandy)	0.25-0.45	trees	0.15-0.18
bare land	0.1-0.35	vegetative surface	0.1-0.25
corregated roof	0.1-0.15	white paint	0.5-0.9
paint (black)	0.05	urban values	0.15-0.18

Table 3: Typical albedo values for surfaces of interest.

Albedo values for a range of relevant surfaces are displayed in Table 3. Evidently white paint is good, black paint and asphalt (very) bad. Note that based on albedo alone vegetative or grass surfaces are no better than bare soil and worse than concrete; it is the evapotranspiration that matters for green roofs.

4 Solution to one-dimensional constant surface temperature model

An exact solution may be found to the problem described above, where the surface conditions are constant. This is achieved by first taking the Laplace transform of the system

$$s\widetilde{T} = \frac{\partial^2 \widetilde{T}}{\partial x^2}$$

subject to

$$\begin{aligned} x = 0: \qquad -\frac{\partial \widetilde{T}}{\partial x} &= \frac{1}{s} - \tilde{T}\,, \\ x \to \infty: \qquad \widetilde{T} &\to 0\,. \end{aligned}$$

The solution in the transformed space is

$$\widetilde{T} = \frac{1}{s(\sqrt{s}+1)} e^{-\sqrt{s}x}\,.$$

This may be back transformed to give

$$T = \text{erfc}\left(\frac{x}{2\sqrt{t}}\right) - e^{(t+x)}\text{erfc}\left(\frac{x}{2\sqrt{t}} + \sqrt{t}\right)\,.$$

The surface temperature is obtained by setting $x = 0$

$$T(0,t) = \left[1 - e^t \text{erfc}\left(\sqrt{t}\right)\right]\,.$$

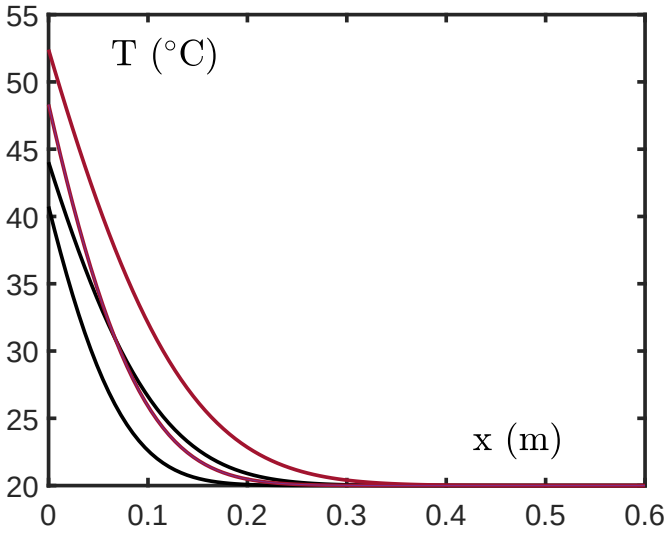

Figure 3: Temperatures at $t = 2, 4$ hours for concrete (black) and soil (red) layers.

In the limit as t becomes large we find

$$T(0,t) = 1 - \frac{1}{\sqrt{\pi t}} - \frac{1}{2\sqrt{\pi t^3}} - \mathcal{O}(t^{-5/2})\,.$$

In Figure 3 we present the predicted temperature profiles in a concrete layer and a soil layer subject to 800 W/m^2 radiation for 2 and 4 hours when no evaporation occurs: all other data is taken from Table 2. The black lines represent concrete, red lines the soil layer. This model predicts that the surface temperature of the soil layer will be some 8°C hotter than the concrete after 4 hours. This is an obvious consequence of the lower albedo value of the soil, permitting more of the suns radiation to be absorbed. We note that grass/vegetation has a similar albedo to soil. In Figure 4 we plot the temperature variation corresponding to the previous case but with evaporation from the soil of 4mm/10 hours. Now the temperature after 4 hours is some 4°C lower in the soil layer than the concrete: this is consistent with what is observed in practice and demonstrates the cooling effect of a green roof.

To emphasise the advantages of having a green roof in Figures In Figures 5 and 6 we plot the variation of surface temperature and energy with time. As time progresses the difference in temperature between a concrete surface and soil becomes increasingly apparent. The difference in energy absorbed is equally impressive, in this example the soil roof absorbs over 20% less than the concrete, which means 20% less energy will be emitted during the night. A layer of vegetation, which would insulate the soil from the sun's rays would decrease the energy absorption even further.

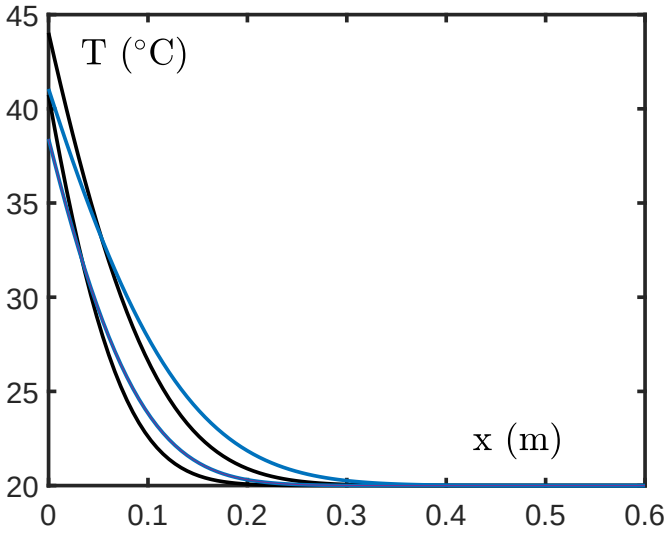

Figure 4: Temperatures at $t = 2, 4$ hours for concrete (black) and soil (blue) layers where evaporation of 4 mm/10 hours is imposed on the soil layer.

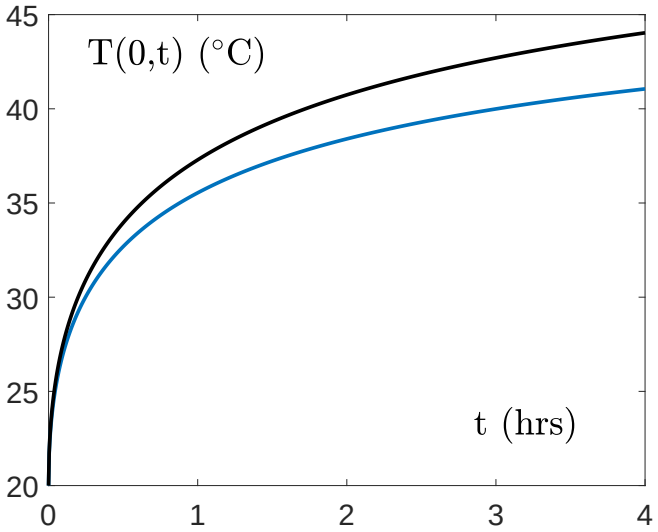

Figure 5: Surface temperature variation for concrete (black) and soil (blue) layers, where evaporation of 4mm/10 hours is imposed on the soil layer.

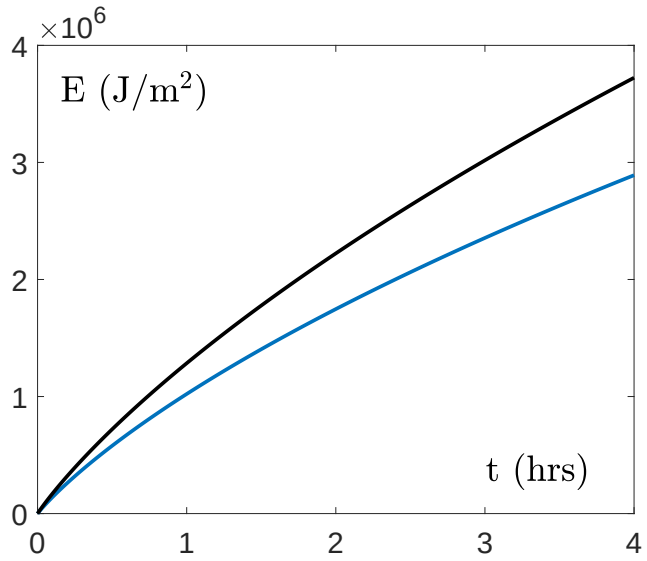

Figure 6: Variation of energy absorbed in the layers for concrete (black) and soil (blue) layers, where evaporation of 4mm/10 hours is imposed on the soil layer.

4.1 Energy absorption

As mentioned earlier, to calculate the temperature field in a city is way beyond the scope of the present study. However, by examining the temperature profile within a layer we are able to calculate the energy absorbed during the day, which then indicates the energy released after sunset.

The (non-dimensional) energy absorbed per unit area is given by

$$E(t) = \int_0^\infty T(x,t)\ dx\ ,$$

where the energy scale is $\rho c L \Delta T$.

The integral may be solved exactly

$$\begin{aligned} I_T &= \int T(x,t)\ dx \\ &= -\mathrm{e}^{t+x}\mathrm{erfc}\left(\frac{x}{2\sqrt{t}}+\sqrt{t}\right) - x\mathrm{erfc}\left(\frac{x}{2\sqrt{t}}\right) + \mathrm{erf}\left(\frac{x}{2\sqrt{t}}\right) + 2\sqrt{\frac{t}{\pi}}\mathrm{e}^{-x^2/4t}\ . \end{aligned}$$

Then the energy is obtained from

$$E(t) = I_T(\infty,t) - I_T(0,t) = \mathrm{e}^t\mathrm{erfc}\left(\sqrt{t}\right) + 2\sqrt{\frac{t}{\pi}} - 1\ .$$

4.2 Dimensional results

The solutions in dimensional form show more clearly the influence of the different parameter values.

The dimensional temperature

$$\begin{aligned} T_d &= \Delta T\, T(x,t) + T_{av} \\ &= T_{av} + \frac{A}{B}\left[\text{erfc}\left(\frac{x_d}{2}\sqrt{\frac{\rho c}{k t_d}}\right) - e^{B(Bt_d/(\rho c)+x_d)/k}\text{erfc}\left(\frac{x_d}{2}\sqrt{\frac{\rho c}{k t_d}} + B\sqrt{\frac{t_d}{\rho c k}}\right)\right] , \end{aligned}$$

where

$$\begin{aligned} A &= (1-\mathcal{A})Q_s - (H + 4\epsilon\sigma T_a^3)(T_{av} - T_a) - \rho L_f \dot{m} , \\ B &= \left(H + 4\epsilon\sigma T_a^3\right) . \end{aligned}$$

The surface temperature

$$T_d(0,t) = T_{av} + \frac{A}{B}\left[1 - e^{B^2 t/(\rho c k)}\text{erfc}\left(B\sqrt{\frac{t}{\rho c k}}\right)\right] .$$

For large times

$$T_d \approx T_{av} + \frac{(1-\mathcal{A})Q_s - (H + 4\epsilon\sigma T_a^3)(T_{av} - T_a) - \rho L_f \dot{m}}{H + 4\epsilon\sigma T_a^3}\left(1 - \sqrt{\frac{\rho c k}{\pi t}}\frac{1}{H + 4\epsilon\sigma T_a^3}\right) ,$$

with a maximum value found by neglecting the final term in the bracket. The parameters of Table 2 indicate the maximum value $\approx 55°$C. However, this asymptotic limit is only approached very slowly. After 10 hours we find a maximum temperature of around 47°C for an average daily temperature of 20°C.

The dimensional energy per unit area

$$E_{dim} = \frac{\rho c k A}{B^2}\left(e^{B^2 t/(\rho c k)}\text{erfc}\left(B\sqrt{\frac{t}{\rho c k}}\right) + 2B\sqrt{\frac{t}{\pi \rho c k}} - 1\right) .$$

4.3 A boundary integral approach

An alternative procedure for finding solutions for the surface temperature and heat flux into the surface is to use a boundary integral approach, now briefly described.

The change in temperature due to a unit heat input per unit surface area (J m^{-2}) at $x = 0$ and $t = 0$ (the Green's function) in a semi-infinite space $x > 0$ is given by

$$\delta T = \frac{1}{\sqrt{\pi \rho c k t}} e^{-x^2/(4\kappa t)}, \text{ where } \kappa = \frac{k}{\rho c},$$

so that due to the heat input rate $Q_{in}(t')$ per unit surface area at $x = 0$ over the time interval $(t', t' + dt')$ the resultant change in temperature within the conductor is given by

$$\delta T = \begin{cases} 0, & \text{for } t < t', \\ \frac{Q_{in}(t')dt'}{\sqrt{\pi\rho ck(t-t')}} e^{-x^2/(4\kappa(t-t')}, & \text{for } t > t'. \end{cases} \tag{8}$$

Adding up all such contributions we get the temperature distribution due to a heat input rate $Q_n(t)$ per unit surface area as

$$T(x,t) = \int_0^t \frac{Q_{in}(t')dt'}{\sqrt{\pi\rho ck(t-t')}} e^{-x^2/(4\kappa(t-t')} dt'. \tag{9}$$

In particular this gives the surface temperature $T_{surf}(t) \equiv T(0,t)$ due to a prescribed heat input rate of $Q_{in}(t)$ (again per unit area) at $x = 0$ as

$$T_{surf}(t) = \int_0^t \frac{Q_{in}(t')}{\sqrt{\pi\rho ck(t-t')}} dt'. \tag{10}$$

In our case the 'external' heat input rate per unit area is simply as defined in (5), with $\dot{d}$ as determined by (1), so this gives

$$T_{surf}(t) = \int_0^t \frac{Q_{in}(T_{surf}(t'), \dot{d}, t')}{\sqrt{\pi\rho ck(t-t')}} dt', . \tag{11}$$

Whilst the external heat flux per unit area Q_{in} is not known a priori as an explicit function of t, its dependence on the surface temperature and t is given by (5). Thus equation (11) represents a consistency requirement on the surface temperature $T_{surf}(t)$.

This is a non-linear Volterra integral equation of the second kind for the surface temperature $T_{surf}(t)$. Once $T_{surf}(t)$ is obtained by solving this equation,the temperature distribution within the conductor can be recovered from (9), and the surface heat flux can also be obtained by direct substitution using (5).

It should be noted that this boundary integral equation contains all the above surface (atmospheric parameters) as well as the below ground parameters, and time variations in radiative input are also captured in this formulation. As such this represents a neat single equation formulation of the problem. Standard numerical equation procedures can be used to extract results. This approach may be especially useful in non-linear heat surface heat transfer rate situations, for example if the wind speed varies from almost zero to large values then the heat transfer regime changes from bouyancy driven free convection regime to a forced convection regime.

As in Section 3 it is sensible to first scale the problem before proceeding to solution. Also as noted earlier in Sections 2 and 3 the expression for Q_{in} is almost linear in T_{surf}, and using this linear approximation leads to a linear Volterra equation which is of the convolution form and can be solved exactly using Laplace Transforms. The results obtained will coincide with those obtained earlier.

5 Conclusions and further work

In this report we have developed two models which permit the calculation of the temperature from the surface to far into the ground. By varying parameters we can replicate heat flow in soil or concrete, there is also the option to include evaporation/evapotranspiration. The results obtained indicate that significant temperature reductions and energy storage in the earth can be achieved by a sensible choice of roof covering and composition. The models are one-dimensional but it is a simple matter to extend the calculations to deal with a patchwork quilt of surfaces as would be present in a city.

Focussing on the effect of albedo alone, white or highly reflective surfaces will absorb the least heat. Due to its colour clean concrete could in fact absorb less heat than soil or green vegetation. In our calculations we compared concrete with an albedo of 0.4 against bare soil with an albedo of 0.2, to find that after 4 hours the soil surface could be almost 10 degrees hotter than the concrete. This leads to greater energy absorption over the day. The albedo value for grass is slightly higher than bare soil, so again we might expect a higher temperature than concrete, however, this is more than offset by evapotranspiration. By adding an evaporation rate of 4mm in 10 hours we found that after 4 hours the soil was some 4 degrees cooler than the concrete. This resulted in a more than 20% reduction in the energy stored in the soil when compared to that in the concrete.

In this preliminary work we simply compared concrete against soil with and without evaporation and were able to demonstrate the reduction in stored energy when evaporation is accounted for. This reduction in energy is due to the fact that a large amount of the incoming solar energy is converted to latent heat, as water is transformed to vapour. The process has two significant consequences: firstly the daytime temperature of the ground will be lower; secondly, there will be less heat released during the night, thus reducing the heat island effect. However, with a vegetative roof the improvements will be even more impressive. Concrete and soil have a high volumetric heat capacity, which means they can store a large amount of energy. A plant layer typically consists of thin strips of vegetation surrounded by air and so has an almost negligible volumetric heat capacity. Plant layers have an albedo similar to that of soil but have the advantageous effects of evapotranspiration and negligible heat capacity. Such a layer, which insulates the ground from the sun's rays, will act to reduce the heat island effect even more than soil.

Evapotranspiration is therefore a key effect in the reduction of heat build-up. It is strongly affected by the wind and relative humidity, so that location is important.

Future work should focus on the following recommendations:

1. The theoretical model should include a layer of vegetation above the soil. This could be treated as a relatively simple extension of the present work to a two layer model.

2. The parameter values used in the Penman-Monteith equation are based on a reference crop of 12cm high sward grass. It would be desirable to have experimental data for the type of plants anticipated for green roofs in the Johannesburg area.

3. The Penman-Monteith model must be adapted so that it permits heat removal due

to natural convection when the wind speed becomes negligible. Currently there is a mismatch between Penman-Monteith and the standard surface boundary condition.

In general terms the addition of vegetation will significantly reduce the urban island effect and the results obtained here quantify this effect. Hopefully this work will help in the process of determining the effectiveness of greening as a tool for improving city conditions.

References

[1] United Nations Department of Economic and Social Affairs, population division, World Urbanization Prospects 2018: Highlights (ST/ESA/SER.A/421).

[2] United Nations, 2004. World Urbanization Prospects: The 2003 Revision. United Nations Publication, New York.

[3] Landsberg H.E. The urban climate, Academic press, London, 1981.

[4] Ashie, Y. Management of Urban heat environment. Urban Environment Management and Technology, vol 1 (2008) 215-238.

[5] Takebayashi, H. and Moriyama, M. Surface heat budget on green roof and high reflection roof for mitigation of urban heat island, Building and Environment vol 42(8) 2007, 2971-2979.

[6] Butera, F. Towards the renewable built environment. In P. Droege (Ed.), Urban energy transition: From fossil fuels to renewable power. Amsterdam: Elsevier, 2008.

[7] Dahl, T. Climate and architecture. London: Routledge. 2010.

[8] Erell, E. Pearlmutter, D. and Williamson, T. Urban microclimate: Designing the spaces between buildings. London: Earthscan, 2011.

[9] Oke, T.R. Towards better scientific communication in urban climate. Theoretical and Applied Climatology, 84(1), 2006, 179-190.

[10] Susca, T., Gaffin, S.R. and Dell'Osso, G.R. Positive effects of vegetation:Urban heat island and green roofs. Environmental pollution, vol 159, 2011, 2119-2126.

[11] Fitchett, A., Govender, P. and Vallabh, P. An exploration of green roofs for indoor and exterior temperature regulation in the South African interior. Environment, Development and Sustainability, 2019. https://doi.org/10.1007/s10668-019-00413-5.

[12] Akbari, H., Rose, S.L. and Taha, H. Analyzing the land cover of an urban environment using high-resolution orthophotos. Lanscape and Urban Planning, vol 63, 2003, 1-14.

[13] Akbari H., Pomerantz M. and Taha H. Cool surfaces and shade trees to reduce energy use and improve air quality in urban areas, Solar Energy, Volume 70, Issue 3, 2001, Pages 295–310, 2001, ISSN 0038–092X, https://doi.org/10.1016/S0038–092X(00)00089–X.

[14] Coakley, J.A. Jr. Reflectance and albedo, surface. In Encyclopedia of the Atmosphere; Holton, J.R., Curry, J.A., Eds.; Academic Press: Cambridge, CA, USA; 2003 pp. 1914–1923.

[15] Taha, H. Urban climates and heat islands: albedo, evapotranspiration, and anthropogenic heat. Energy and buildings, 25(2),1997, 99–103.

[16] Sodoudi, S., Shahmohamadi, P., Vollack, K., Cubasch, U., and Che–Ani, A.I. Mitigating the urban heat island effect in megacity Tehran. Advances in Meteorology, 2014.

[17] Adinna, E., Christian, E.I., and Okolie, A.T. Assessment of urban heat island and possible adaptations in Enugu urban using landsat–ETM. Journal of Geography and Regional Planning, 2(2),2009, 30-36.

[18] Synnefa, A., Dandou, A., Santamouris, M., Tombrou, M., and Soulakellis, N. On the use of cool materials as a heat island mitigation strategy. Journal of Applied Meteorology and Climatology, 47(11), 2008, 2846–2856.

[19] Yamamoto, Y. Measures to mitigate urban heat islands. Science and Technology Trends Quarterly Review, 18(1), 2006, 65–83.

[20] Oke, T.R. The energetic basis of the urban heat island. Quarterly Journal of the Royal Meteorological Society, 108(455), 1982, 1–24.

[21] Quattrochi, D.A., Luvall, J.C., Rickman, D.L., Estes, M.G., Laymon, C.A. and Howell, B.F. A decision support information system for urban landscape management using thermal infrared data: Decision support systems. Photogrammetric Engineering and Remote Sensing, 66(10), 2000, 1195–1207.

[22] Bennett, M and Saab, A.E. Modelling of the urban heat island and of its interaction with pollutant dispersal, Atmospheric Environment (1967), Volume 16, Issue 8, 1982, Pages 1797-1822, ISSN 0004-6981, https://doi.org/10.1016/0004–6981(82)90369–9.

[23] Atkinson, B. Numerical Modelling of Urban Heat–Island Intensity. Boundary–Layer Meteorology. 109. 285–310. 10.1023/A:1025820326672, 2003.

[24] Giannaros, T.M., Melas, D., Daglis, I.A., Keramitsoglou, I. and Kourtidis, K. Numerical study of the urban heat island over Athens (Greece) with the WRF model, Atmospheric Environment, Volume 73, 2013, Pages 103–111, ISSN 1352–2310, https://doi.org/10.1016/j.atmosenv.2013.02.055.

[25] Nazarian, N., Sin, T. and Norford, L. Numerical modeling of outdoor thermal comfort in 3D, Urban Climate, Volume 26, 2018, Pages 212–230, ISSN 2212–0955, https://doi.org/10.1016/j.uclim.2018.09.001.

[26] Meili, N., Manoli, G., Burlando, P., Bou–Zeid, E., Chow, W.T.L., Coutts, A.M., Daly, E., Nice, K.A., Roth, M., Tapper, N.J., Velasco, E., Vivoni, E.R., and Fatichi, S.: An urban ecohydrological model to quantify the effect of vegetation on urban climate and hydrology (UT& C v1.0), Geosci. Model Dev., 13, 335–362, https://doi.org/10.5194/gmd–13–335–2020, 2020.

[27] Najmaddin, P.M., Whelan M.J. and Balzter, H. Estimating daily reference evapotranspiration in a semi-arid region using remote sensing data. Remote Sens. 9, 2017, 779; doi:10.3390/rs9080779.

[28] Nuruzzaman, M. Urban heat island: effects and mitigation measures- a review. International Journal of Environmental Monitoring and Analysis. 3(2): 2015, 67-73.

[29] Chen, Mao-Liang, Bhowmick, S. and Mallick, R.B. Harvesting energy from asphalt pavements and reducing the heat island effect, 2008.

[30] Myrup, L.O. A numerical model of the urban heat island. Journal of Applied Meteorology. Vol 8, 1969, 908-918.

[31] Thermal mass http://www.greenspec.co.uk/building-design/thermal-mass/.

[32] Rosseland, S. Theoretical Astrophysics. Clarenden Press 1936.

[33] Siegel, R. and Howell, J. R. Thermal radiation heat transfer. 4th edn. Taylor and Francis-Hemisphere, 2001.

[34] O'Tool, J.O. and Tomar, V. S. Transpiration, leaf temperature and water potential of rice and barnyard grass in a flooded field, Agricultural Meteorology Vol 26, Issue 4, 1982.

[35] Jarvis, P.G. The interpretation of the variations in leaf water potential and stomatal conductance found in canopies in the field. Philosophical Transactions of the Royal Society B. 273 (927): 1976, 593–610.

[36] Kotak, Y., Gul, M.S., Muneer, T. and Ivanova, S.M. Investigating the Impact of Ground Albedo on the Performance of PV Systems. CIBSE Technical Symposium, London, UK, 16-17 April 2015.

[37] Monteith, J.L. Evaporation and environment. Symposia of the Society for Experimental Biology. 19: 1965, 205–224.

[38] Doorenbos, J. and W. Pruitt. 'FAO-24, Irrigation and drainage Paper NO 24: Crop Water Requirements (1977) (available online).

[39] Alduchov, O.A. and Eskridge, R.E. Improved magnus form approximation of saturation vapor pressure. Journal of Applied Meteorology. 35 (4): 1996, 601–9.

[40] Sinnot, R.K. Chemical Engineering Design, Butterworth-Heinemann, 2005, p 331.

[41] Zhang, R. and Jiang, L. The albedo of pervious cement concrete linearly decreases with porosity. Advances in Materials Science and Engineering 2015, Article ID 746592, http://dx.doi.org/10.1155/2015/746592